



HTRA1 expression is associated with immune-cell infiltration and survival in breast cancer

Dawei Zhao¹, Wanfeng Li¹, Yan Wang¹, Gengyue Zhang², Xinhua Bai³, Hong Yu^{2^*}

¹Department of Breast Cancer, Jilin Cancer Hospital, Changchun, China; ²Jilin Province Institute of Cancer Prevention and Treatment, Jilin Cancer Hospital, Changchun, China; ³Department of Pathology, Jilin Cancer Hospital, Changchun, China

Contributions: (I) Conception and design: D Zhao, H Yu; (II) Administrative support: D Zhao, H Yu; (III) Provision of study materials or patients: D Zhao, H Yu; (IV) Collection and assembly of data: H Yu, D Zhao, W Li, Y Wang, G Zhang; (V) Data analysis and interpretation: All authors; (VI) Manuscript writing: All authors; (VII) Final approval of manuscript: All authors.

Correspondence to: Hong Yu, MM. Jilin Province Institute of Cancer Prevention and Treatment, Jilin Cancer Hospital, No. 1018 Huguang Road, Chaoyang District, Changchun 130012, China. Email: yhzhy@126.com.

Background: High temperature requirement A1 (HTRA1), a member of the HTRA family, is a serine peptidase involved in many crucial bioprocesses such as proliferation, mitochondrial homeostasis, apoptosis, and protein quality control. It also plays an important role in the development of various tumors. However, the potential role and mechanisms of action of HTRA1 in breast cancer (BRCA) remain unclear. We conducted a bioinformatics-based study to investigate *HTRA1* expression in BRCA alongside its associations with immune-cell infiltrates and survival outcomes.

Methods: The expression of *HTRA1* in BRCA samples was analyzed using RNAseq datasets from The Cancer Genome Atlas and Gene Expression Omnibus. R software was employed to assess the relationship between HTRA1 expression and clinicopathological characteristics, tumor-infiltrating immune cells, and immunity-associated biomarkers in BRCA. MethSurv and cBioPortal database were utilized to evaluate DNA methylation and genovariation within the HTRA1 DNA. Receiver operating characteristic curves, Kaplan-Meier analysis, and Cox regression were performed to estimate the impact of HTRA1 on diagnosis, prognosis, and response to chemotherapy in BRCA.

Results: *HTRA1* expression was significantly downregulated in BRCA tissues compared to adjacent normal breast tissue controls. Differentially expressed genes associated with *HTRA1* expression primarily enriched in cell proliferation pathways. Furthermore, altered *HTRA1* expression significantly correlated with patient age, tumor histological type, T stage, progesterone receptor/estrogen receptor status, and PAM50 subtype of BRCA. Both positive and negative associations were observed between *HTRA1* levels and the abundance of different types of immune cells, as well as immune biomarkers, including resting mast cells, follicular helper T cells, PD-L1, p53, and Ki67. Low *HTRA1* expression was related with pathological complete response in luminal B BRCA patients undergoing chemotherapy. Additionally, lower *HTRA1* expression in BRCA was associated with inferior overall survival and relapse-free survival.

Conclusions: *HTRA1* expression is associated with immune-cell infiltration, response to chemotherapy, and survival outcomes in BRCA. HTRA1 has the potential to serve as a promising biomarker and therapeutic target moving forward.

Keywords: Breast cancer (BRCA); high temperature requirement A1 (HTRA1); DNA methylation; tumor-infiltrating immune cells; prognosis

Submitted May 09, 2023. Accepted for publication Oct 18, 2023. Published online Dec 19, 2023.

doi: 10.21037/tcr-23-773

View this article at: <https://dx.doi.org/10.21037/tcr-23-773>

^{*} ORCID: 0000-0002-6819-6607.

Introduction

Breast cancer (BRCA) is currently the most frequently diagnosed cancer type and one of the leading causes of cancer-related deaths among women worldwide (1). In clinical practice, immunohistochemical staining for estrogen receptor (ER), progesterone receptor (PR), and erb-b2 receptor tyrosine kinase 2 (ERBB2)/human epidermal growth factor receptor 2 (HER2) are utilized as diagnostic markers to categorize BRCA into luminal A, luminal B, HER2-enriched (non-luminal), and basal [triple-negative breast cancer (TNBC)] subtypes (2). Advances in early detection, treatment, and promising therapeutic opportunities have significantly improved the clinical outcomes and survival rates of BRCA patients (3,4). However, the heterogeneity of BRCA subtypes contributes to varying clinicopathological characteristics, treatment options, prognoses, and recurrence patterns (5).

The composition of immune cells within the BRCA microenvironment plays a crucial role in disease progression and clinical outcome. Innate immune cells (macrophages, neutrophils, dendritic cells, innate lymphoid cells, myeloid-derived suppressor cells, and natural killer cells) and adaptive immune cells (T cells and B cells) within this microenvironment contribute cooperatively to tumor progression and therapeutic response (6). Therefore, elucidating the intricate interplay between molecular

characteristics of BRCA and multiple immune cells within the tumor microenvironment can lead to favorable outcomes.

High temperature requirement A (HTRA) proteases are a family of serine proteases involved in various cellular processes (7), among which HTRA1 is the first identified and extensively studied member (8). It plays a crucial role in several fundamental physiological and pathological processes, such as cell proliferation and invasion, and cell adhesion (9). Current studies on HTRA1 generally support its role as a tumor suppressor. Decreased HTRA1 expression is associated with poor prognosis in ovarian cancer (10), metastatic melanoma (11), prostate cancer (12), lung cancer (13), endometrial cancer (14), and BRCA (15). However, the mechanisms underlying the effects of decreased HTRA1 expression and its role in tumor immune-cell infiltration, immune checkpoints, diagnosis, and prognosis of BRCA have not been fully elucidated. In this study, we conducted a comprehensive bioinformatics analysis utilizing The Cancer Genome Atlas (TCGA) (<https://portal.gdc.cancer.gov/>) and Gene Expression Omnibus (GEO) (<https://www.ncbi.nlm.nih.gov/geo/>) to assess the important effects of HTRA1 in BRCA (16). We present this article in accordance with the STREGA reporting checklist (available at <https://tcr.amegroups.com/article/view/10.21037/tcr-23-773/rc>).

Methods

The study was conducted in accordance with the Declaration of Helsinki (as revised in 2013).

Data collection

The RNAseq data in the Fragments Per Kilobase per Million format (level 3 HTSeq-FPKM) and the corresponding clinicopathological information of 1,222 samples (1,109 BRCA and 113 normal breast tissue samples, August 2021) were downloaded from the Breast Invasive Carcinoma Project in TCGA. Then the FPKM format data were converted into transcripts per million (TPM) reads for subsequent analysis. Two BRCA datasets, GSE109169 (<https://www.ncbi.nlm.nih.gov/geo/query/acc.cgi?acc=GSE109169>) (17) and GSE10780 (<https://www.ncbi.nlm.nih.gov/geo/query/acc.cgi?acc=GSE10780>) (18) from GEO database were also downloaded for validation of *HTRA1* expression. GSE109169 was used to assess the gene expression profiles of 25 paired normal breast and tumor tissues based on the detection platform GPL5175

Highlight box

Key findings

- Decreased high temperature requirement A1 (HTRA1) expression was found to be significantly associated with breast cancer (BRCA) and inferior survival of patients.

What is known and what is new?

- Previous studies on HTRA1 generally support its role as a tumor suppressor. However, contrasting findings also exist.
- Here, we report associations between *HTRA1* expression and abundance of different types of tumor-associated immune cells and immuno-biomarkers in BRCA, including resting mast cells, follicular helper T cells, PD-L1, *TP53*, and *Ki67*. *HTRA1* levels were also correlated to BRCA subtype, response to therapy, and survival.

What is the implication, and what should change now?

- The potential value of HTRA1 in BRCA is achieved by regulating tumor cell proliferation and tumor immunity. HTRA1 serves as a potential therapeutic target and prognostic biomarker. Further investigations would be necessary to depict the complicated regulatory effects of HTRA1 in BRCA in future.

(HuEx-1_0-st) Affymetrix Human Exon 1.0 ST Array [transcript (gene) version]. GSE10780 was used to analyze the gene expression profiles of 143 normal breast tissues and 42 BRCA tissues based on the detection platform GPL570 (HG-U133_Plus_2) Affymetrix Human Genome U133 Plus 2.0 Array.

Analysis of HTRA1 mRNA expression level in BRCA and normal breast tissue samples

The expression level of *HTRA1* mRNA was firstly compared with data from 33 types of human cancer extracted from TCGA (19). For TCGA-BRCA datasets, we further analyzed *HTRA1* mRNA expression in tumor samples and their paired normal controls based on BRCA subtypes. The data of *HTRA1* extracted from GSE109169 and GSE10780 datasets were used to validate TCGA-BRCA results. Then the TCGA-BRCA samples were divided into high- and low-*HTRA1* expression group based on the median expression of *HTRA1*. Differentially expressed genes (DEGs) between the two groups were screened out and analyzed by “DESeq2” (v1.26.0) R package (20) with log fold change absolute value >1.5 and P value <0.05 as a threshold. The volcano plot and heat map of the DEGs were visualized using the “ggplot2” (v3.3.3) R package.

Functional enrichment analysis of HTRA1-associated DEGs in BRCA

The “ClusterProfiler” (v3.14.3) R package (21) was used for the functional annotation and Gene Set Enrichment Analysis (GSEA) (22) for the selected DEGs. The curated reference gene sets c2. cp.v7.2. symbols.gmt from MSigDB (<http://www.gsea-msigdb.org/gsea/msigdb>) were designated for GSEA (23). We identified significantly enriched clusters using false discovery rate (FDR) <0.25 and $P_{\text{adjust}} < 0.05$ as a threshold. A protein-protein interaction (PPI) analysis was performed using the STRING database (24) and visualized by Cytoscape software (v3.9.1) (25). The interaction threshold was set to 0.4.

Correlation analysis between HTRA1 expression, immune-cell infiltration, and immuno-related biomarkers in BRCA

The ssGSEA algorithm in the “GSVA” (v1.34.0) R package (26) was used to evaluate the tumor infiltration status of 24 types of immune cell (27). Spearman correlation analysis was performed to determine the relationship between *HTRA1*

expression, immune-cell infiltration status, and immunity-related biomarkers. Among them, *PDCD1* [programmed cell death protein 1 (PD-1)], *CD274* [programmed cell death ligand 1 (PD-L1)], *CTLA4* and *LAG3* are important immune checkpoint markers that are associated with tumor immune escape (28); *TIGIT*, *HAVCR2*, *LAYN*, and *CXCL3* are T cell exhaustion markers; *IFNG* [interferon γ (IFN- γ)], *IL2* [interleukin 2 (IL-2)], *GZMB* (granzyme B), and *PRF1* (perforin) are T cell effector function markers. *TP53* is a tumor suppressor (29). *MKI67* (Ki67) is a proliferation marker.

Analysis of HTRA1 genovariation and DNA methylation in the CpG islands of HTRA1 DNA in BRCA samples

The genomic variation in *HTRA1* gene was analyzed by cBioPortal database (<https://www.cbioportal.org/>) (30,31) including eight BRCA datasets: TCGA (19), METABRIC (32), INSERM (33), MBC project (<https://mbcproject.org/>), BCCRC (34), Broad (35), MSKCC (36), and Sanger (37). Kaplan-Meier survival analysis and log-rank test were performed to determine the prognostic significance of the genomic variation in *HTRA1* gene. The DNA methylation in the CpG sites of *HTRA1* gene and their prognostic values were analyzed by MethSurv database (<https://biit.cs.ut.ee/methsurv/>) (38). The association between CpG methylation of *HTRA1* DNA and the overall survival (OS) of BRCA patients was also evaluated.

Correlation analysis between HTRA1 expression and the clinicopathological characteristics of BRCA patients

The clinicopathological information of BRCA patients was extracted from TCGA-BRCA (39). The differences of various clinicopathological parameters were compared between the high- and low-*HTRA1* expression group by the Shapiro-Wilk normality test, Kruskal-Wallis test, and Dunn’s multiple hypothesis test. The results were corrected by the Bonferroni method and visualized using the “ggplot2” (v3.3.3) R package. Logistic regression analysis was used to evaluate the relationship between *HTRA1* expression and the clinicopathological characteristics of BRCA patients.

Evaluation of the prognostic significance of HTRA1 expression in BRCA patients and their therapeutic response

The survival data of BRCA patients from TCGA-BRCA (39)

and GEO (16,40) were analyzed by the “survival” (v3.2-10) and “survminer” (v0.4.9) R package. Kaplan–Meier survival analysis as well as univariate and multivariate Cox regression were conducted to determine the survival of BRCA patients based on *HTRA1* expression. The diagnostic and time-dependent survival ROC curve were generated using the “pROC” (v1.17.0.1) and “timeROC” (v0.4) R package. The online tool ROC Plotter (<http://www.rocplot.org/site/index>) was used to evaluate the impact of *HTRA1* expression on the therapeutic response of breast patients from GEO (41).

Statistical analysis

The differences in *HTRA1* expression between groups were analyzed using the Wilcoxon signed-rank test and one-way ANOVA. The correlations between *HTRA1* expression and clinicopathological characteristics of patients were assessed using Fisher’s exact test, Chi-squared test, Wilcoxon signed-rank test, and logistic regression. Other statistical analyses were detailed above. $P < 0.05$ was considered to be statistically significant.

Results

HTRA1 expression was significantly dysregulated in multiple types of cancer including BRCA

Figure 1A shows *HTRA1* expression in 33 types of cancer in TCGA. The mRNA level of *HTRA1* was found to be downregulated in seven types of cancer (BLCA: $P = 0.003$; BRCA: $P = 0.003$, shown also in *Figure 1B*; CESC: $P = 0.004$; KICH: $P < 0.001$; KIRP: $P < 0.001$; PRAD: $P < 0.001$, and UCEC: $P < 0.001$), and upregulated in eight types of cancer (CHOL: $P = 0.003$; ESCA: $P = 0.002$; HNSC: $P < 0.001$; KIRC: $P < 0.001$; LIHC: $P < 0.001$; PCPG: $P = 0.015$; STAD: $P < 0.001$, and THCA: $P < 0.001$). *HTRA1* mRNA expression in breast tumor tissues was also assessed using data from GSE109169 and GSE10780 datasets (*Figure 1C, 1D*, respectively). The comparative results showed that *HTRA1* mRNA expression in tumor tissues was significantly lower than that in normal breast tissues ($P_{\text{adj}} = 0.0233$, $P_{\text{adj}} = 0.0111$).

Figure 1E–1H shows *HTRA1* expression in tumor tissues and their matched normal controls from TCGA-BRCA by subtype. *HTRA1* expression was significantly lower in Basal-like BRCA than that in the paired normal tissues ($n = 16$), while it was not significantly different for either HER2 positive ($n = 9$) or luminal B BRCA ($n = 21$), but was significantly higher for luminal A BRCA ($n = 56$).

The median *HTRA1* expression value was used to classify TCGA-BRCA samples into high- and low-*HTRA1* expression group. Using the absolute log fold change > 1.5 and $P < 0.05$ as a threshold, we screened out 607 DEGs (74 upregulated and 533 downregulated) in the high-*HTRA1* expression group compared to the low-*HTRA1* expression group (*Figure 1I*). The ten most significant DEGs are shown in the single gene co-expression heat map in *Figure 1J*.

Furthermore, the immunohistochemical results from Human Protein Atlas (<https://www.proteinatlas.org/>) (42,43) verified the expression of HTRA1 protein. In 17 out of 23 samples, HTRA1 staining was absent in breast tumor cells, whereas its weak staining was observed in the cytoplasm or cytomembrane of tumor cells in the remaining six samples (*Tables S1, S2*).

HTRA1-associated DEGs in BRCA were mainly involved in cell proliferation and cell cycle process

The functional enrichment annotation for the *HTRA1*-associated DEGs in BRCA was conducted by the “clusterProfiler” R package. The results of Gene Ontology (GO) and Kyoto Encyclopedia of Genes and Genomes (KEGG) pathway enrichment, encompassing highly enriched biological process, cellular component, and molecular function ($P < 0.05$), are displayed in *Figure 2A* and *Table S3*. The most enriched biological process were extracellular structure organization, extracellular matrix organization, and antimicrobial humoral response. Collagen-containing extracellular matrix, nucleosome, and collagen trimer emerged as the most enriched cellular component. Regarding molecular function, ion channel activity, extracellular matrix structural constituent, and collagen binding exhibited the highest levels of enrichment. The top-ranked KEGG pathways included neuroactive ligand-receptor interaction, alcoholism, and protein digestion and absorption. The PPI network of the DEGs revealed an association between *HTRA1* and other genes (*Figure 2B* and *Figure S1*). GSEA analysis demonstrated that *HTRA1*-associated DEGs were significantly enriched in cell proliferation-related clusters (*Figure 2C–2I*), such as M phase (NES = -1.600 , $P_{\text{adj}} = 0.036$, FDR = 0.032), G2/M checkpoints (NES = -1.729 , $P_{\text{adj}} = 0.036$, FDR = 0.032), G0 and early G1 (NES = -1.733 , $P_{\text{adj}} = 0.037$, FDR = 0.033), cell cycle checkpoints (NES = -1.737 , $P_{\text{adj}} = 0.036$, FDR = 0.032), cell cycle (NES = -1.625 , $P_{\text{adj}} = 0.036$, FDR = 0.032; NES = -1.640 , $P_{\text{adj}} = 0.036$, FDR = 0.032), and DNA replication (NES = -1.731 , $P_{\text{adj}} = 0.036$, FDR = 0.032). *HTRA1*-associated DEGs were also enriched in cellular

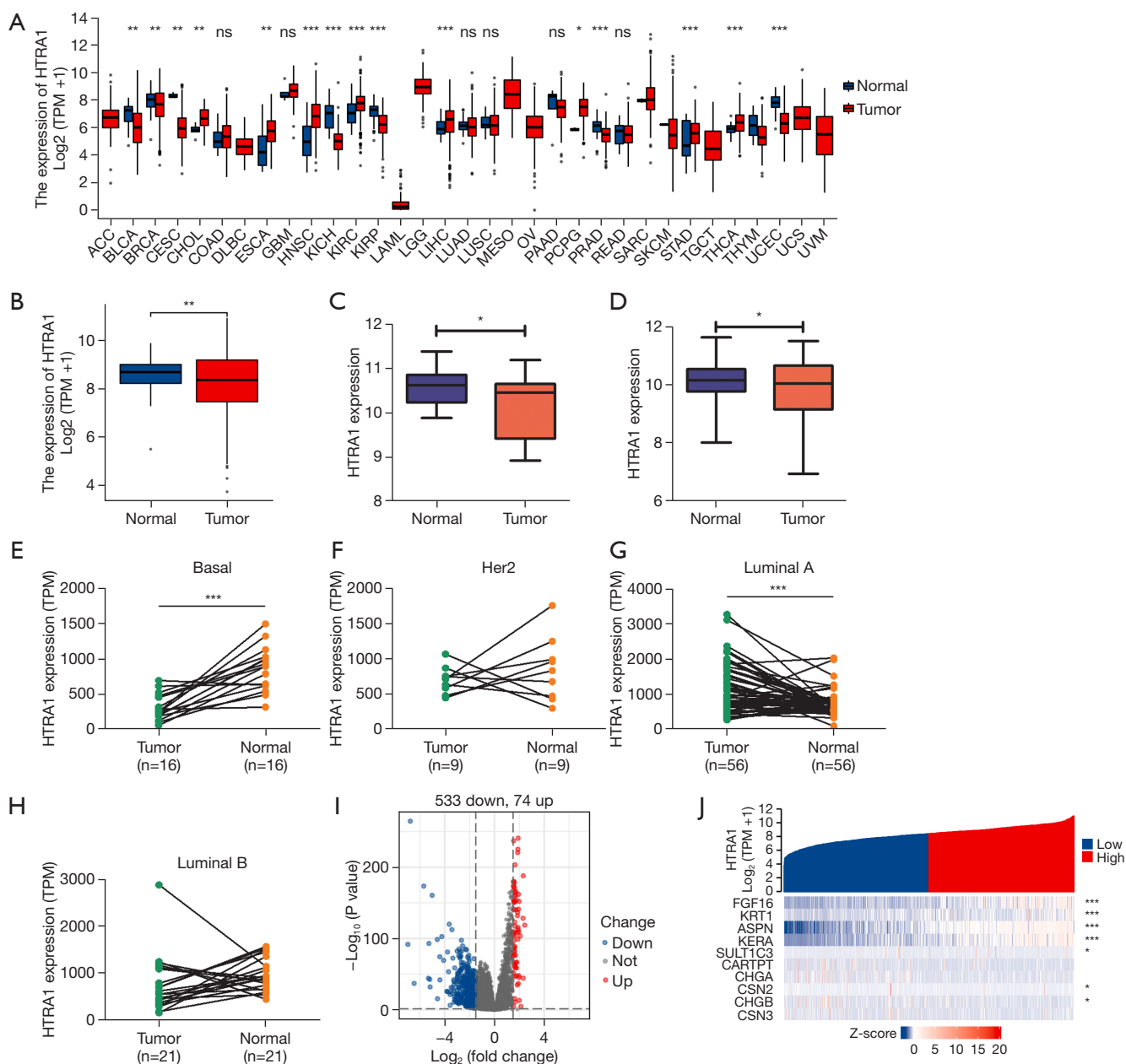


Figure 1 Expression of *HTRA1* is significantly dysregulated in BRCA and other cancer types. (A) *HTRA1* expression in 33 types of cancer compare with their corresponding adjacent normal tissues. ns, $P \geq 0.05$; *, $P < 0.05$; **, $P < 0.01$; ***, $P < 0.001$. Wilcoxon rank sum test. (B) *HTRA1* expression was significantly lower in the BRCA tissues compared to the adjacent peritumoral normal breast tissues in TCGA-BRCA. (C,D) *HTRA1* expression was significantly lower in breast tumor tissues as compared to the normal breast tissues in (C) GSE109169 (paired samples) and (D) GSE10780. (E-H) Differential expression of *HTRA1* in BRCA tissues and matched normal samples from TCGA-BRCA by subtype: Basal, $P < 0.001$; HER2, $P = 0.4368$; Luminal A, $P < 0.001$, and Luminal B, $P = 0.1448$. Paired-sample *t*-test, two-tailed. (I) Volcano plot of DEGs associated with *HTRA1* expression. Every dot corresponds to a gene. The red and dark blue dots represent significant DEGs, and the red dots indicate upregulated expression, dark blue dots indicate downregulated expression, and black dots indicate DEGs with no significant difference. (J) Heat map (top 10 DEGs) showed the level of DEGs in TCGA-BRCA with high- and low-*HTRA1* expression divided by the median *HTRA1* level. HTRA1, high temperature requirement A1; HER2, human epidermal growth factor receptor 2; ACC, adrenocortical cancer; BLCA, bladder urothelial carcinoma; BRCA, breast cancer; CESC, cervical squamous cell carcinoma and endocervical adenocarcinoma; CHOL, cholangiocarcinoma; COAD, colon adenocarcinoma; DLBC, lymphoid neoplasm diffuse large B-cell lymphoma; ESCA, esophageal carcinoma; GBM, glioblastoma multiforme; HNSC, head and neck squamous cell carcinoma; KICH, kidney chromophobe; KIRC, kidney renal clear cell carcinoma; KIRP, kidney renal papillary cell carcinoma, LAML, acute myeloid leukemia; LGG, lower grade glioma, LIHC, Liver hepatocellular carcinoma; LUAD, lung adenocarcinoma; LUSC, lung squamous cell carcinoma, MESO, mesothelioma; OV, ovarian serous cystadenocarcinoma; PAAD, pancreatic adenocarcinoma; PCPG, pheochromocytoma and paraganglioma; PRAD, Prostate adenocarcinoma; READ, rectal adenocarcinoma; SARC, sarcoma, SKCM, skin cutaneous melanoma; STAD, stomach adenocarcinoma; TGCT, testicular germ cell tumors; THCA, thyroid cancer; THYM, thymoma; UCEC, uterine corpus endometrioid cancer; UCS, uterine carcinosarcoma; UVM, uveal melanoma.

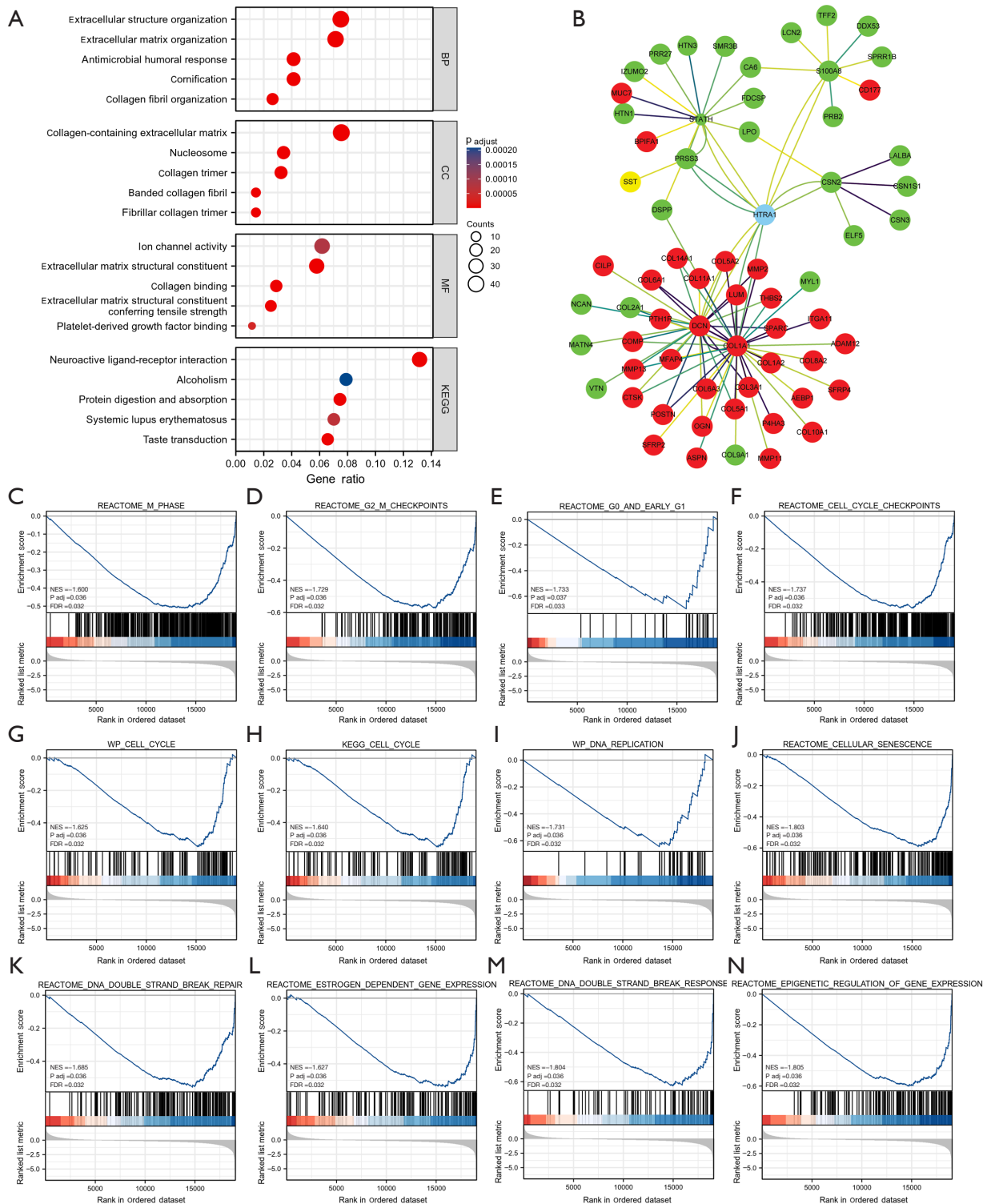


Figure 2 Functional enrichment results of the *HTRA1*-associated DEGs in BRCA. (A) GO and KEGG enrichment analysis of *HTRA1*-associated DEGs showed the enriched BP, CC, and MF. (B) The PPI network of the DEGs. Lines represent protein-protein interaction. The larger the circle, the more the interaction between genes. Red, in the high-*HTRA1* expression group, log fold change value >1.5. Green, in the low-*HTRA1* expression group, log fold change value <-1.5. (C-N) GSEA analysis showed the altered signaling pathway in BRCA based on *HTRA1*-associated DEGs. HTRA1, high temperature requirement A1; DEG, differentially expressed gene; BRCA, breast cancer; GO, Gene Ontology; KEGG, Kyoto Encyclopedia of Genes and Genomes; BP, biological process; CC, cellular component; MF, molecular function; PPI, protein-protein interaction; GSEA, gene set enrichment analysis.

senescence (NES = -1.803, P_{adj} = 0.036, FDR = 0.032), DNA double strand break repair (NES = -1.685, P_{adj} = 0.036, FDR = 0.032), estrogen dependent gene expression (NES = -1.627, P_{adj} = 0.036, FDR = 0.032), DNA double strand break response (NES = -1.804, P_{adj} = 0.036, FDR = 0.032), and epigenetic regulation of gene expression (NES = -1.805, P_{adj} = 0.036, FDR = 0.032) (Figure 2J-2N).

HTRAI expression was correlated with the infiltration of multiple immune cells in BRCA tissues

HTRAI showed a negative correlation with aDC (R = -0.114, $P < 0.001$) and Th2 cells (R = -0.228, $P < 0.001$), but a positive correlation with CD8 T cells (R = 0.201, $P < 0.001$), cytotoxic cells (R = 0.091, $P = 0.003$), DC (R = 0.137, $P < 0.001$), eosinophils (R = 0.267, $P < 0.001$), iDC (R = 0.485, $P < 0.001$), macrophages (R = 0.316, $P < 0.001$), mast cells (R = 0.590, $P < 0.001$), neutrophils (R = 0.333, $P < 0.001$), NK CD56bright cells (R = 0.140, $P < 0.001$), NK CD56dim cells (R = 0.063, $P = 0.035$), NK cells (R = 0.537, $P < 0.001$), pDC (R = 0.195, $P < 0.001$), T cells (R = 0.091, $P = 0.002$), Tcm (R = 0.081, $P = 0.007$), Tem (R = 0.191, $P < 0.001$), TFH (R = 0.099, $P < 0.001$), Tgd (R = 0.169, $P < 0.001$), and Th1 cells (R = 0.164, $P < 0.001$) (Figure 3A). The tumor infiltration levels of neutrophils, cytotoxic cells, DC, aDC, NK, and Th2 cells in the high- and low-*HTRAI* expression group were consistent with the Spearman analysis results (Figure 3B-3G).

Regarding immune cell markers, *HTRAI* expression was positively correlated with specific biomarkers for CD8⁺ T cells (*CD8A*, *CD8B*), TFH (*BCL6*), Th1 (*T-bet/TBX21*, *STAT4*), Th2 (*CCR3*, *GATA3*, *STAT5A*, *STAT6*), Th9 (*IRF4*, *PU.1/SPI1*, *TGFBR2*), Th17 (*IL-21R*, *IL-23R*, *STAT3*), Th22 (*AHR*, *CCR10*), Treg (*CCR8*, *FOXP3*), M1 macrophage (*COX2/PTGS2*, *INOS/NOS2*), M2 macrophage (*CD206/MRC1*, *CD115/CSF1R*), and TAM (*PDCD1LG2*, *CD80*, *CD40*); whereas it was negatively correlated with biomarkers for B cells (*CD38*), Th1 (*IL2RB2*), and Th17 (*IL-17A*) in BRCA (Table S4).

HTRAI expression was correlated with immuno-related markers, TP53, and Ki67 in BRCA

In BRCA tissues, *HTRAI* expression showed a positive correlation with the levels of *CD274* (PD-L1), *TIGIT*, *HAVCR2*, *LAYN*, *IL2* (IL-2), *PRF1* (perforin), and *TP53*. Additionally, it exhibited a negative correlation with the levels of *LAG3*, *GZMB* (granzyme B), and *MKI67* (Ki-67) (Figure 4).

HTRAI genovariation had no impact on the survival of BRCA patients

Only 1% genovariation was observed in *HTRAI* based on data from eight BRCA datasets, including TCGA (n = 1,084), METABRIC (n = 2,509), INSERM (n = 216), MBC project (n = 237), BCCRC (n = 65), Broad (n = 103), MSKCC (n = 70), and Sanger (n = 100) (Figure 5A). Kaplan-Meier survival curve and log-rank test results showed that there was no significant difference in OS ($P = 0.726$), progression free survival ($P = 0.456$), relapse free status ($P = 0.543$), disease free survival ($P = 0.430$), and disease-specific survival (DSS) ($P = 0.400$) between patients with or without *HTRAI* genovariation (Figure 5B-5F). Further analysis revealed the incidence of *HTRAI* mutation was 0.42% in MBC project, 0.46% in INSERM, and 0.37% in TCGA BRCA samples, respectively (Figure 5G). The highest level of *HTRAI* amplification was observed in the MBC project dataset (2.53%), followed by METABRIC and TCGA (both 0.74%) and INSERM (0.46%). The mRNA expression level of *HTRAI* showed a slight increase in tumors with amplified *HTRAI* gene compared to those with diploid status (median, 11.7013 vs. 11.4394) (Figure 5H).

HTRAI DNA methylation affected the prognosis of BRCA patients

In the *HTRAI* DNA, there were 13 CpG islands showed aberrant DNA methylation, including cg05723130, cg15868400, cg06777002, cg07863439, cg15719652, cg01145353, cg09553346, cg17875153, cg05426956, cg22701672, cg00701951, cg03974204, and cg23791011 (Figure 6). Moreover, the methylation levels of seven CpG islands, namely cg00701951, cg01145353, cg01962937, cg04768425, cg06474225, cg15719652, and cg26466234, were associated with the prognosis of BRCA (Table 1). Increased methylation levels in these seven CpG islands, particularly cg01145353, cg15719652, and cg00701951, were associated with poorer OS in BRCA patients.

HTRAI expressions correlated with multiple clinicopathological characteristics in BRCA

Table 2 displays the association between *HTRAI* expression and clinicopathological characteristics in BRCA patients. Significant differences were observed between the high- and low-*HTRAI* expression group in

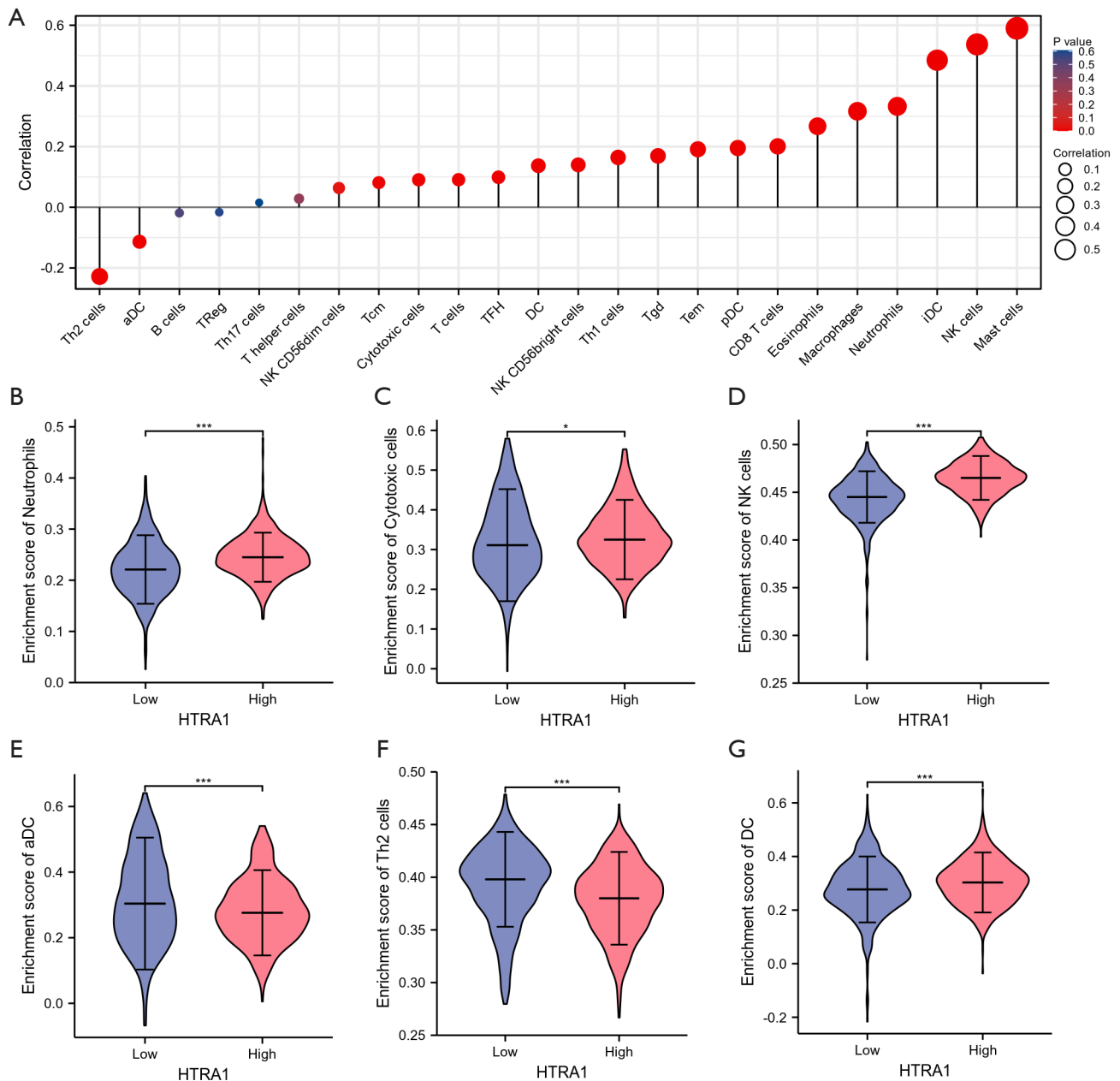


Figure 3 The correlation between immune-cell infiltration and *HTRA1* expression in BRCA. (A) Spearman analysis result showed the correlation between the infiltration of 24 types of immune cells and *HTRA1* expression in BRCA tissues. (B-G) The infiltration level of (B) neutrophils, (C) cytotoxic cells, (D) NK cells, (E) aDC, (F) Th2 cells, and (G) DC in the high- and low-*HTRA1* expression group. *, $P < 0.05$; ***, $P < 0.001$. *HTRA1*, high temperature requirement A1; BRCA, breast cancer; aDC, activated DC; TReg, regulatory T cells; Th17 cells, type 17 Th cells; NK, natural killer cells; Tem, T central memory; TFH, T follicular helper; DC, dendritic cells; Th1 cells, type 1 Th cells; Tgd, T gamma delta; Tem, T effector memory; pDC, plasmacytoid DC; iDCs, immature DCs; Th2 cells, type 2 Th cells.

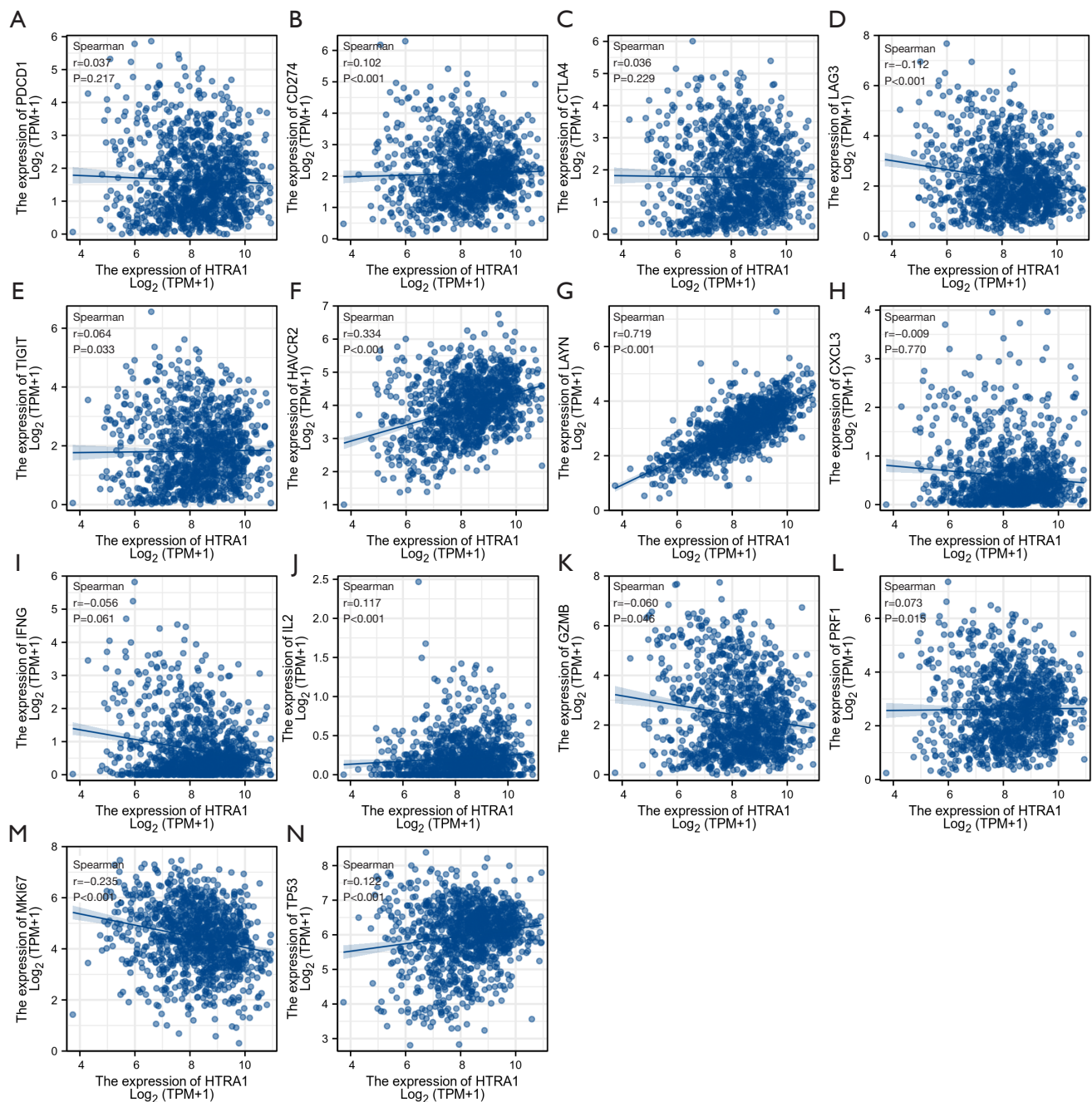


Figure 4 The correlation between *HTRA1* expression and immuno-related markers in BRCA (Spearman correlation). (A-D) Correlation of *HTRA1* expression and immune checkpoint marker *PDCD1* (PD-1), *CD274* (PD-L1), *CTLA4* and *LAG3*. (E-H) Correlation of *HTRA1* expression and T cell exhaustion marker *TIGIT*, *HAVCR2*, *LAYN*, and *CXCL3*. (I-L) Correlation of *HTRA1* expression and T cell effector function marker *IFNG* (IFN- γ), *IL2* (IL-2), *GZMB* (granzyme B), and *PRF1* (perforin). (M) Correlation of *HTRA1* expression and *MKI67* (Ki-67). (N) Correlation of *HTRA1* expression and *TP53*. *HTRA1*, high temperature requirement A1; BRCA, breast cancer; *PDCD1* (PD-1), programmed cell death 1; PD-L1, programmed cell death 1 ligand 1; *CTLA4*, cytotoxic T-lymphocyte associated protein 4; *LAG3*, lymphocyte activating 3; *TIGIT*, T cell immunoreceptor with Ig and ITIM domains; *HAVCR2*, hepatitis A virus cellular receptor 2; *LAYN*, layilin; *CXCL3*, C-X-C motif chemokine ligand 3; *IFNG* (IFN- γ), interferon gamma; *IL-2*, interleukin 2; *GZMB*, granzyme B; *PRF1* (perforin), perforin 1; *MKI67* (Ki67), marker of proliferation Ki-67; *TP53*, tumor protein p53.

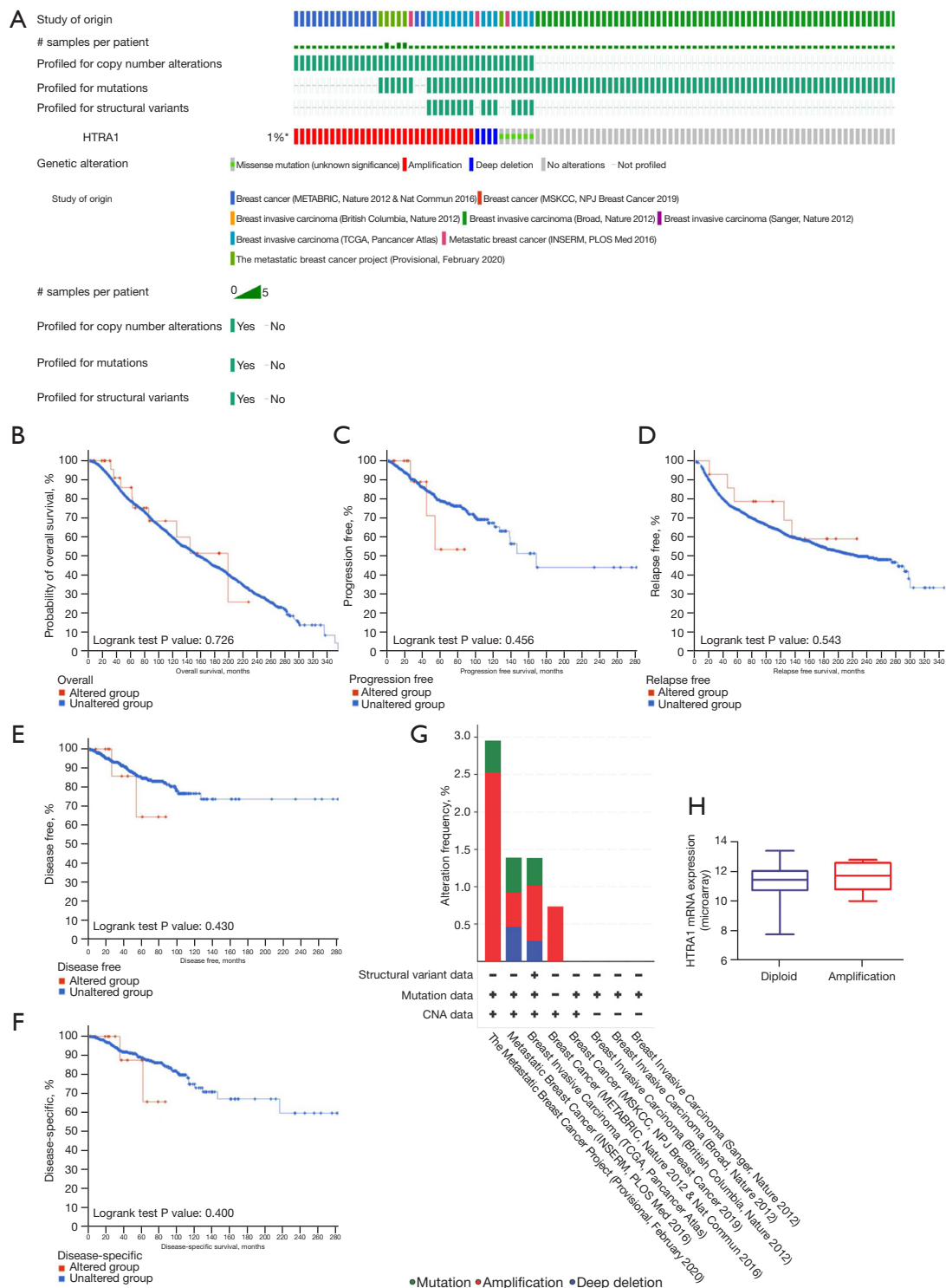


Figure 5 *HTRA1* genovariation has no impact on *HTRA1* expression in breast cancer. (A) OncoPrint visual summary depicted the *HTRA1* genovariation. *, not all samples were profiles (altered / profiled =40/3,989). (B-F) Kaplan-Meier survival curve showed (B) overall survival, (C) progression free survival, (D) relapse free status, (E) disease free survival, and (F) disease-specific survival of BRCA patients with altered or unaltered *HTRA1* genovariation. (G) *HTRA1* genetic alteration in different datasets deposited in cBioPortal. (H) Comparison of *HTRA1* expression in BRCA patients of diploid and amplified *HTRA1* in METABRIC (n=2,509, Mann-Whitney *t*-test, P=0.2057). *HTRA1*, high temperature requirement A1; BRCA, breast cancer; CNA, copy-number alterations.

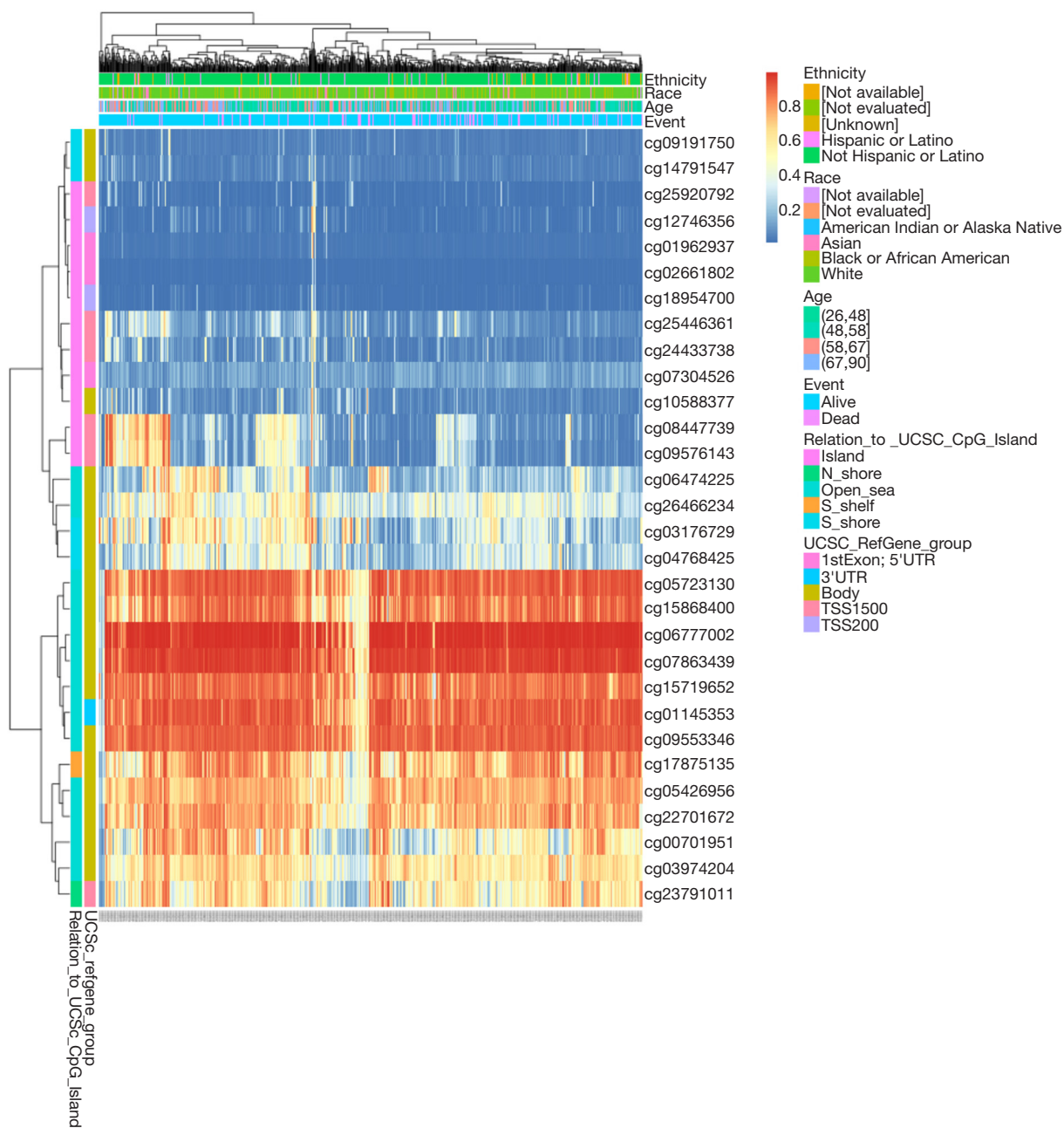


Figure 6 Heat map displayed DNA methylation status in HTRA1 DNA in BRCA tissues. HTRA1, high temperature requirement A1; BRCA, breast cancer.

terms of clinical T stage, histological type, PR status, ER status, PAM50 subtype, and age. Additionally, *HTRA1* expression also varied significantly with age, pathologic stage, histological type, T stage, N stage, ER status, PR status, and PAM50 subtype in BRCA (Figure 7). Logistic regression analysis further confirmed a positive correlation of *HTRA1* expression with N stage, age, ER

status, PR status, histological type, and PAM50 subtype in BRCA (Table 3).

High HTRA1 expression was associated with favorable prognosis of BRCA patients from GEO datasets, but not TCGA

Kaplan-Meier survival curves demonstrated that the

Table 1 Effect of DNA methylation status in the CpG sites of HTRA1 DNA on the prognosis of BRCA patients

CpG island	Hazard ratio	P value
Body-Open_Sea-cg00701951	0.557	0.022
3'UTR-Open_Sea-cg01145353	0.599	0.015
1stExon;5'UTR-Island-cg01962937	0.514	0.0013
1stExon;5'UTR-Island-cg02661802	0.718	0.14
Body-S_Shore-cg03176729	0.816	0.38
Body-Open_Sea-cg03974204	0.713	0.089
Body-S_Shore-cg04768425	0.526	0.0021
Body-Open_Sea-cg05426956	1.519	0.11
Body-Open_Sea-cg05723130	1.151	0.57
Body-Open_Sea-cg06474225	0.543	0.0059
Body-Open_Sea-cg06777002	1.397	0.2
1stExon;5'UTR-Island-cg07304526	0.593	0.055
Body-Open_Sea-cg07863439	1.391	0.2
TSS1500-Island-cg08447739	0.828	0.46
Body-S_Shore-cg09191750	0.817	0.37
Body-Open_Sea-cg09553346	0.775	0.27
TSS1500-Island-cg09576143	0.646	0.11
Body-Island-cg10588377	1.359	0.21
TSS200-Island-cg12746356	0.668	0.11
Body-S_Shore-cg14791547	1.449	0.083
Body-Open_Sea-cg15719652	0.561	0.0039
Body-Open_Sea-cg15868400	1.408	0.099
Body-S_Shelf-cg17875135	1.252	0.26
TSS200-Island-cg18954700	0.753	0.16
Body-Open_Sea-cg22701672	0.756	0.16
TSS1500-N_Shore-cg23791011	0.909	0.69
TSS1500-Island-cg24433738	0.899	0.59
TSS1500-Island-cg25446361	1.13	0.54
TSS1500-Island-cg25920792	0.804	0.28
Body-Open_Sea-cg26466234	0.476	0.0065

HTRA1, high temperature requirement A1; BRCA, breast cancer.

relative *HTRA1* expression level (high or low) in TCGA-BRCA patients was not correlated with OS (P=0.776), DSS (P=0.551), or progression-free interval (PFI, P=0.446). However, when examining the GEO database (2017,

n=5,143, HTRA1 Affymetrix ID is 201185_at) (40,44), high *HTRA1* expression was associated with favorable OS and relapse-free survival (RFS) in BRCA patients (Figure 8), indicating a significantly reduced risk for recurrence and death.

Furthermore, our ROC curves indicated that *HTRA1* expression may not have diagnostic value in distinguishing tumor from adjacent normal tissue [area under the curve (AUC) =0.572]. Additionally, we used the online tool ROC Plotter to assess the impact of *HTRA1* expression on therapeutic response in BRCA patients from GEO (41). The selected datasets were all from clinical trials including GSE16446 (NCT00017095, NCT00336791), GSE41998 (NCT00455533), GSE50948 (ISRCTN86043495), GSE66305 (NCT00429299), and GSE16391 (NCT00004205). The results showed that for the luminal B subtype, patients with lower *HTRA1* expression had a higher likelihood of achieving pathological complete response to chemotherapy (Figure 9 and Table S5).

Discussion

By evaluating *HTRA1* expression in human cancers within TCGA database, we observed dysregulation of *HTRA1* in 15 out of 33 types of cancer. Specifically, in BRCA, both TCGA and GEO datasets showed a significant reduction in *HTRA1* expression in tumor tissues. However, low *HTRA1* expression was associated with an unfavorable prognosis in patients from GEO, but not TCGA. These results are consistent with previous studies. Wang *et al.* reported a notable decrease or absence of HTRA1 expression in *in situ* or invasive ductal BRCA tissues compared to its prominent expression in normal breast ductal epithelium tissues (45). Lehner *et al.* measured *HTRA1* mRNA expression in 131 BRCA patients (15) and found significantly higher levels of *HTRA1* in lower tumor stage, which correlated with longer OS and disease free survival. Franco *et al.* evaluated 66 sentinel node positive BRCA cases and discovered a negative correlation between HTRA1 expression and metastasis development as well as local relapse (46). However, a retrospective analysis suggested that six epithelial mesenchymal transition genes including *LUM*, *SFRP4*, *COL6A3*, *MMP2*, *CXCL12*, and *HTRA1* were continuously expressed at higher levels in samples from patients with metastatic BRCA (47). We also observed a significant correlation between *HTRA1* expression in BRCA tissues and various factors such as age, clinical N stage, histological type, PR status, ER status,

Table 2 The clinicopathological characteristics of BRCA patients with high- and low-*HTRA1* expression

Characteristic	Low expression of <i>HTRA1</i> (n=541)	High expression of <i>HTRA1</i> (n=542)	P value
T stage, n (%)			0.014
T1	115 (10.6)	162 (15)	
T2	331 (30.6)	298 (27.6)	
T3	72 (6.7)	67 (6.2)	
T4	20 (1.9)	15 (1.4)	
N stage, n (%)			0.054
N0	278 (26.1)	236 (22.2)	
N1	168 (15.8)	190 (17.9)	
N2	49 (4.6)	67 (6.3)	
N3	37 (3.5)	39 (3.7)	
M stage, n (%)			1.000
M0	457 (49.6)	445 (48.3)	
M1	10 (1.1)	10 (1.1)	
Pathologic stage, n (%)			0.587
Stage I	85 (8)	96 (9.1)	
Stage II	321 (30.3)	298 (28.1)	
Stage III	116 (10.9)	126 (11.9)	
Stage IV	9 (0.8)	9 (0.8)	
Age, n (%)			0.016
≤60 years	280 (25.9)	321 (29.6)	
>60 years	261 (24.1)	221 (20.4)	
Histological type, n (%)			<0.001
Infiltrating ductal carcinoma	412 (42.2)	360 (36.8)	
Infiltrating lobular carcinoma	64 (6.6)	141 (14.4)	
PR status, n (%)			<0.001
Negative	232 (22.4)	110 (10.6)	
Indeterminate	3 (0.3)	1 (0.1)	
Positive	278 (26.9)	410 (39.7)	
ER status, n (%)			<0.001
Negative	179 (17.3)	61 (5.9)	
Indeterminate	2 (0.2)	0 (0)	
Positive	333 (32.2)	460 (44.4)	
HER2 status, n (%)			0.165
Negative	275 (37.8)	283 (38.9)	
Indeterminate	7 (1)	5 (0.7)	
Positive	65 (8.9)	92 (12.7)	
PAM50, n (%)			<0.001
Normal	12 (1.1)	28 (2.6)	
LumA	193 (17.8)	369 (34.1)	
LumB	128 (11.8)	76 (7)	
Her2	45 (4.2)	37 (3.4)	
Basal	163 (15.1)	32 (3)	

HTRA1, high temperature requirement A1; BRCA, breast cancer; PR, progesterone receptor; ER, estrogen receptor; HER2, human epidermal growth factor receptor 2; PAM50, prediction analysis of microarray 50; LumA, luminal A; LumB; luminal B.

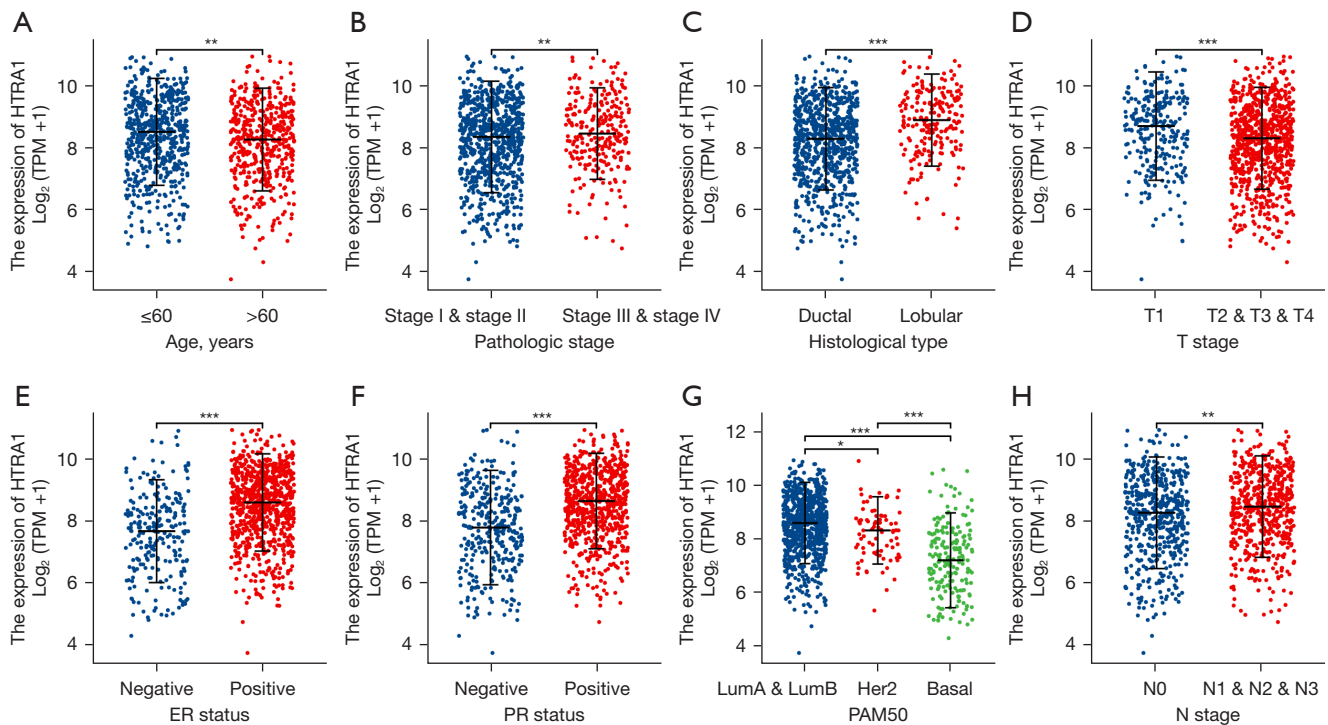


Figure 7 *HTRA1* expression correlated with multiple clinicopathological characteristics of BRCA patients. (A-H) The correlation between *HTRA1* expression and age (A), pathologic stage (B), histological type (C), T stage (D), ER (E), PR (F), PAM50 (G), and N stage (H) of BRCA patients. *, P<0.05; **, P<0.01, ***, P<0.001. *HTRA1*, high temperature requirement A1; BRCA, breast cancer; PR, progesterone receptor; ER, estrogen receptor; HER2, human epidermal growth factor receptor 2; PAM50, prediction analysis of microarray 50; LumA, luminal A; LumB; luminal B.

Table 3 Logistic regression analysis of the relationship between the clinicopathological characteristics and *HTRA1* expression in BRCA patients

Characteristics	Total (N)	Odds ratio (OR)	P value
T stage (T3 & T4 vs. T1 & T2)	1,080	0.864 (0.624–1.196)	0.379
N stage (N1 & N2 & N3 vs. N0)	1,064	1.373 (1.079–1.748)	0.010
M stage (M1 vs. M0)	922	1.027 (0.418–2.526)	0.953
Pathologic stage (stage III & IV vs. stage I & II)	1,060	1.113 (0.841–1.473)	0.454
Age (>60 vs. ≤60 years)	1,083	0.739 (0.581–0.939)	0.013
Histological type (infiltrating lobular carcinoma vs. infiltrating ductal carcinoma)	977	2.521 (1.825–3.516)	<0.001
PR status (positive vs. negative)	1,030	3.111 (2.372–4.098)	<0.001
ER status (positive vs. negative)	1,033	4.054 (2.950–5.634)	<0.001
HER2 status (positive vs. negative)	715	1.375 (0.963–1.974)	0.081
Radiation therapy (yes vs. no)	987	1.062 (0.826–1.366)	0.639
Menopause status (peri & post vs. pre)	972	0.862 (0.640–1.159)	0.326
PAM50 (Basal vs. LumA & LumB & HER2)	1,043	0.149 (0.098–0.220)	<0.001

HTRA1, high temperature requirement A1; BRCA, breast cancer; PR, progesterone receptor; ER, estrogen receptor; HER2, human epidermal growth factor receptor 2; PAM50, prediction analysis of microarray 50; LumA, luminal A; LumB; luminal B.

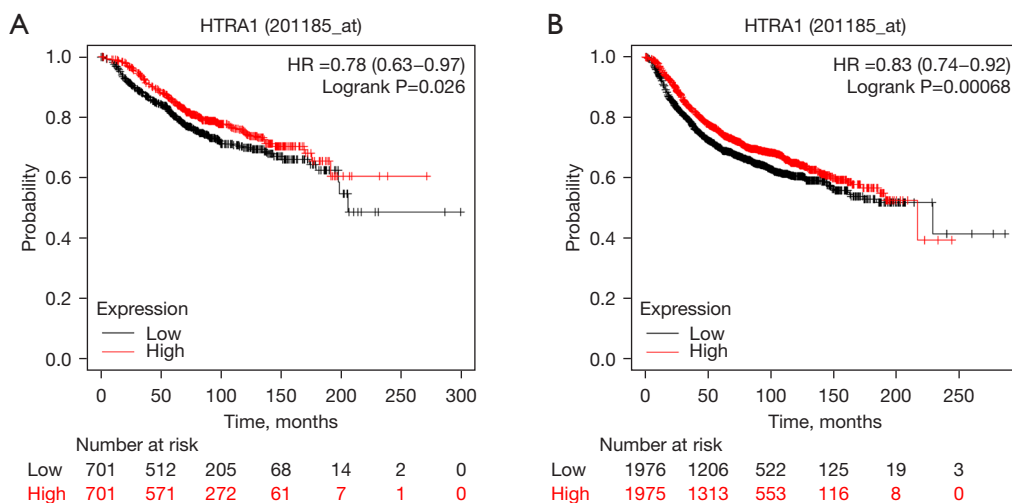


Figure 8 The result of KM-plotter analysis showed the impact of *HTRA1* expression on breast patients' survival. (A) Overall survival (n=1,402); (B) relapse-free survival (n=3,951). HTRA1, high temperature requirement A1; KM, Kaplan-Meier; HR, hazard ratio.

and PAM50 subtype. However, it is important to note that *HTRA1* expression exhibits high heterogeneity among different BRCA subtypes. This finding requires further investigation due to limitations in sample size and variations in sampling sites and procedures.

Subsequently, we screened for 607 *HTRA1*-related DEGs from TCGA-BRCA samples based on median *HTRA1* expression. These DEGs primarily participate in extracellular matrix organization processes and exhibit molecular functions related to these processes. GSEA results demonstrated that the *HTRA1*-related DEGs were predominantly involved in cell proliferation, cell cycle regulation, cellular senescence, and the estrogen-dependent gene expression clusters. Wang *et al.* also reported decreased *HTRA1* expression in BRCA cell lines (45). *HTRA1* siRNA-transfected non-tumorigenic MCF10A normal breast epithelium cells exhibited smaller size, increased growth rate, as well as enhanced migration and invasion capabilities. Protease nexin-1 (PN-1) promotes cancer cell metastasis by remodeling the tumor matrix. Tang *et al.* demonstrated that upregulated PN-1 in BRCA promotes cell invasion, migration, and stemness through the EGF/EGFR/PKC δ /MEK/ERK/EGR1 axis, with *HTRA1* being a target of PN-1. Consequently, *HTRA1* overexpression inhibits migration and invasion of BRCA cells, while PN-1 overexpression nullifies this inhibitory effect (48). Collectively, these findings confirm the inhibitory impact of *HTRA1* on cell proliferation in breast cells. Nevertheless, there are discrepancies among studies, and the current

evidence does not definitively establish *HTRA1* as a tumor suppressor (9).

Genetic variation has been implicated in the diagnosis, treatment, and prognosis of BRCA patients (49). However, in our analyses, *HTRA1* genovariation was not found to be correlated with survival of BRCA patients. We hypothesize that this may be due to the minimal impact of genovariation on *HTRA1* expression. DNA methylation is an epigenetic mechanism which plays a crucial role in tumorigenesis. Alterations in *HTRA1* DNA methylation can affect its expression in BRCA (15). Notably, there is an inverse correlation between mRNA expression and DNA methylation at the transcription start site of the *HTRA1* promoter in BRCA cells (45). In our assessment of the relationship between *HTRA1* DNA methylation and prognosis of BRCA patients, we observed that increased methylation at three CpG islands (cg01145353, cg15719652, and cg00701951) was associated with poorer OS compared to decreased methylation.

The immune contexture within the breast tumor microenvironment can influence tumor growth and metastasis. A previous study evaluated tumor-infiltrating lymphocytes (TILs) and their relevance to therapeutic response and prognosis in 3,771 patients with primary BRCA undergoing neoadjuvant chemotherapy (50). The results demonstrated that increased TIL density predicted chemotherapy response across all BRCA subtypes. Furthermore, TIL density was associated with a survival benefit in HER2-positive and TNBC patients (50). Our

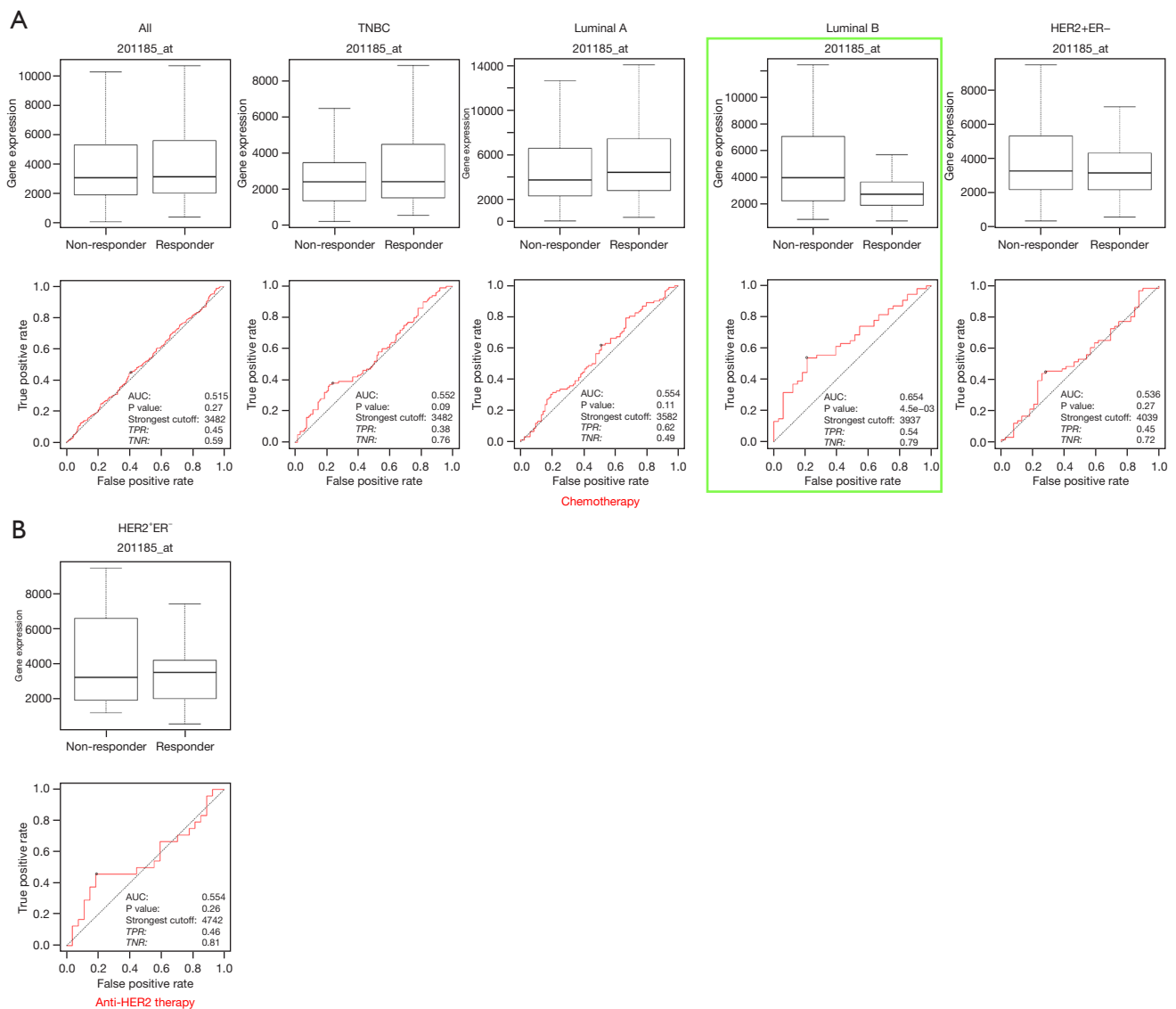


Figure 9 The ROC curves showed the differential *HTRA1* expression between breast cancer patients with or without pathological complete response to chemotherapy and anti-HER2 therapy. (A) Chemotherapy; (B) anti-HER2 therapy. *HTRA1*, high temperature requirement A1; ER, estrogen receptor; HER2, human epidermal growth factor receptor 2; TNBC, triple-negative breast cancer.

study revealed potential correlations between *HTRA1* expression and the proportion of tumor-infiltrating cells, as well as immune cell markers such as *CD8A*, *CCR3*, *GATA3*, and *STAT6*. Additionally, significant associations were found between *HTRA1* expression and the immune checkpoint PD-L1, T cell exhaustion marker, T cell effector function marker, *TP53*, and Ki67. These findings support the potential suppressive role of *HTRA1* in BRCA. Recent studies have investigated the use of anti-PD-1/PD-L1 agents in BRCA, similar to melanoma or non-small cell

lung cancer, particularly in TNBC. Encouraging outcomes have been observed with monotherapy or combination treatment (51). The signature of exhausted T cells can also predict immunotherapy response in BRCA (52). Therefore, our results suggest that *HTRA1* may serve as a potential target to enhance the efficacy of immunotherapy in BRCA patients.

Folgueira *et al.* identified predictive markers for neoadjuvant chemotherapy response in BRCA patients (53). They highlighted a trio of genes, including *HTRA1*,

CLPTM1, and *MTSS1* genes, which could accurately differentiate responsive from non-responsive tumors. Another study involving 333 non-metastatic locally advanced BRCA patients who received neoadjuvant chemotherapy demonstrated that higher *HTRA1* expression was associated with increased recurrence risk and cancer-related death (54). Our findings indicate that *HTRA1* expression can only discriminate between responsive and non-responsive Luminal B patients undergoing chemotherapy. However, the utility of *HTRA1* as a biomarker for BRCA prognosis and treatment response requires further comprehensive understanding.

There were some limitations in our study. Firstly, we solely analyzed *HTRA1* expression in BRCA samples from TCGA and GEO public database, and it would be beneficial to validate our findings using clinical samples. Secondly, we did not directly assess the molecular mechanism and activity of *HTRA1* through *in vitro* and *in vivo* experiments, therefore our hypothesis about the effects of genetic variation, expression levels, and progression/prognosis/response to therapy are speculative. Thirdly, the relationships between *HTRA1* expression and the function of tumor-infiltrating immune cells within the breast tumor microenvironment needs to be elucidated through well-designed studies. Further investigations are necessary to unravel the complex regulatory role of *HTRA1* in BRCA.

Conclusions

In conclusion, our analysis revealed a significant decrease in *HTRA1* expression in BRCA datasets. Our findings suggest that *HTRA1* may exert its influence on BRCA development through the modulation of genes involved in tumor cell proliferation and immunity. Additionally, we observed that *HTRA1* expression might play a crucial role in chemotherapy response and DNA methylation. Thus, *HTRA1* expression is associated with BRCA prognosis. Collectively, these findings propose *HTRA1* as a potential therapeutic target and a useful prognostic biomarker in BRCA.

Acknowledgments

Funding: This work was supported by the Jilin Province Health Science and Technology Capability Improvement Project (grant No. 2021LC127 to D.Z.).

Footnote

Reporting Checklist: The authors have completed the STREGA reporting checklist. Available at <https://tcr.amegroups.com/article/view/10.21037/tcr-23-773/rc>

Peer Review File: Available at <https://tcr.amegroups.com/article/view/10.21037/tcr-23-773/prf>

Conflicts of Interest: All authors have completed the ICMJE uniform disclosure form (available at <https://tcr.amegroups.com/article/view/10.21037/tcr-23-773/coif>). The authors have no conflicts of interest to declare.

Ethical Statement: The authors are accountable for all aspects of the work in ensuring that questions related to the accuracy or integrity of any part of the work are appropriately investigated and resolved. The study was conducted in accordance with the Declaration of Helsinki (as revised in 2013).

Open Access Statement: This is an Open Access article distributed in accordance with the Creative Commons Attribution-NonCommercial-NoDerivs 4.0 International License (CC BY-NC-ND 4.0), which permits the non-commercial replication and distribution of the article with the strict proviso that no changes or edits are made and the original work is properly cited (including links to both the formal publication through the relevant DOI and the license). See: <https://creativecommons.org/licenses/by-nc-nd/4.0/>.

References

1. Sung H, Ferlay J, Siegel RL, et al. Global Cancer Statistics 2020: GLOBOCAN Estimates of Incidence and Mortality Worldwide for 36 Cancers in 185 Countries. *CA Cancer J Clin* 2021;71:209-49.
2. Sørlie T, Perou CM, Tibshirani R, et al. Gene expression patterns of breast carcinomas distinguish tumor subclasses with clinical implications. *Proc Natl Acad Sci U S A* 2001;98:10869-74.
3. Ye F, Dewanjee S, Li Y, et al. Advancements in clinical aspects of targeted therapy and immunotherapy in breast cancer. *Mol Cancer* 2023;22:105.
4. Huppert LA, Gumusay O, Idossa D, et al. Systemic therapy for hormone receptor-positive/human epidermal growth factor receptor 2-negative early stage and metastatic breast

- cancer. *CA Cancer J Clin* 2023;73:480-515.
5. Szymiczek A, Lone A, Akbari MR. Molecular intrinsic versus clinical subtyping in breast cancer: A comprehensive review. *Clin Genet* 2021;99:613-37.
 6. Qayoom H, Sofi S, Mir MA. Targeting tumor microenvironment using tumor-infiltrating lymphocytes as therapeutics against tumorigenesis. *Immunol Res* 2023;71:588-99.
 7. Wang Y, Nie G. Overview of Human HtrA Family Proteases and Their Distinctive Physiological Roles and Unique Involvement in Diseases, Especially Cancer and Pregnancy Complications. *Int J Mol Sci* 2021;22:10756.
 8. Zumbunn J, Trueb B. Primary structure of a putative serine protease specific for IGF-binding proteins. *FEBS Lett* 1996;398:187-92.
 9. Altobelli E, Marzioni D, Lattanzi A, et al. HtrA1: Its future potential as a novel biomarker for cancer. *Oncol Rep* 2015;34:555-66.
 10. Chien J, Staub J, Hu SI, et al. A candidate tumor suppressor HtrA1 is downregulated in ovarian cancer. *Oncogene* 2004;23:1636-44.
 11. Baldi A, De Luca A, Morini M, et al. The HtrA1 serine protease is down-regulated during human melanoma progression and represses growth of metastatic melanoma cells. *Oncogene* 2002;21:6684-8.
 12. Welsh JB, Sapinoso LM, Su AI, et al. Analysis of gene expression identifies candidate markers and pharmacological targets in prostate cancer. *Cancer Res* 2001;61:5974-8.
 13. Esposito V, Campioni M, De Luca A, et al. Analysis of HtrA1 serine protease expression in human lung cancer. *Anticancer Res* 2006;26:3455-9.
 14. Mullany SA, Moslemi-Kebria M, Rattan R, et al. Expression and functional significance of HtrA1 loss in endometrial cancer. *Clin Cancer Res* 2011;17:427-36.
 15. Lehner A, Magdolen V, Schuster T, et al. Downregulation of serine protease HTRA1 is associated with poor survival in breast cancer. *PLoS One* 2013;8:e60359.
 16. Barrett T, Wilhite SE, Ledoux P, et al. NCBI GEO: archive for functional genomics data sets--update. *Nucleic Acids Res* 2013;41:D991-5.
 17. Chang JW, Kuo WH, Lin CM, et al. Wild-type p53 upregulates an early onset breast cancer-associated gene GAS7 to suppress metastasis via GAS7-CYFIP1-mediated signaling pathway. *Oncogene* 2018;37:4137-50.
 18. Chen DT, Nasir A, Culhane A, et al. Proliferative genes dominate malignancy-risk gene signature in histologically-normal breast tissue. *Breast Cancer Res Treat* 2010;119:335-46.
 19. Hoadley KA, Yau C, Hinoue T, et al. Cell-of-Origin Patterns Dominate the Molecular Classification of 10,000 Tumors from 33 Types of Cancer. *Cell* 2018;173:291-304.e6.
 20. Love MI, Huber W, Anders S. Moderated estimation of fold change and dispersion for RNA-seq data with DESeq2. *Genome Biol* 2014;15:550.
 21. Yu G, Wang LG, Han Y, et al. clusterProfiler: an R package for comparing biological themes among gene clusters. *OMICS* 2012;16:284-7.
 22. Subramanian A, Tamayo P, Mootha VK, et al. Gene set enrichment analysis: a knowledge-based approach for interpreting genome-wide expression profiles. *Proc Natl Acad Sci U S A* 2005;102:15545-50.
 23. Liberzon A, Birger C, Thorvaldsdóttir H, et al. The Molecular Signatures Database (MSigDB) hallmark gene set collection. *Cell Syst* 2015;1:417-25.
 24. Szklarczyk D, Gable AL, Nastou KC, et al. The STRING database in 2021: customizable protein-protein networks, and functional characterization of user-uploaded gene/ measurement sets. *Nucleic Acids Res* 2021;49:D605-12.
 25. Shannon P, Markiel A, Ozier O, et al. Cytoscape: a software environment for integrated models of biomolecular interaction networks. *Genome Res* 2003;13:2498-504.
 26. Hänzelmann S, Castelo R, Guinney J. GSEA: gene set variation analysis for microarray and RNA-seq data. *BMC Bioinformatics* 2013;14:7.
 27. Bindea G, Mlecnik B, Tosolini M, et al. Spatiotemporal dynamics of intratumoral immune cells reveal the immune landscape in human cancer. *Immunity* 2013;39:782-95.
 28. Ibrahim R, Saleh K, Chahine C, et al. LAG-3 Inhibitors: Novel Immune Checkpoint Inhibitors Changing the Landscape of Immunotherapy. *Biomedicine* 2023;11:1878.
 29. Wang H, Guo M, Wei H, et al. Targeting p53 pathways: mechanisms, structures, and advances in therapy. *Signal Transduct Target Ther* 2023;8:92.
 30. Cerami E, Gao J, Dogrusoz U, et al. The cBio cancer genomics portal: an open platform for exploring multidimensional cancer genomics data. *Cancer Discov* 2012;2:401-4.
 31. Gao J, Aksoy BA, Dogrusoz U, et al. Integrative analysis of complex cancer genomics and clinical profiles using the cBioPortal. *Sci Signal* 2013;6:pl1.
 32. Pereira B, Chin SF, Rueda OM, et al. The somatic mutation profiles of 2,433 breast cancers refines their

- genomic and transcriptomic landscapes. *Nat Commun* 2016;7:11479.
33. Lefebvre C, Bachelot T, Filleron T, et al. Mutational Profile of Metastatic Breast Cancers: A Retrospective Analysis. *PLoS Med* 2016;13:e1002201.
 34. Shah SP, Roth A, Goya R, et al. The clonal and mutational evolution spectrum of primary triple-negative breast cancers. *Nature* 2012;486:395-9.
 35. Banerji S, Cibulskis K, Rangel-Escareno C, et al. Sequence analysis of mutations and translocations across breast cancer subtypes. *Nature* 2012;486:405-9.
 36. Nixon MJ, Formisano L, Mayer IA, et al. PIK3CA and MAP3K1 alterations imply luminal A status and are associated with clinical benefit from pan-PI3K inhibitor buparlisib and letrozole in ER+ metastatic breast cancer. *NPJ Breast Cancer* 2019;5:31.
 37. Stephens PJ, Tarpey PS, Davies H, et al. The landscape of cancer genes and mutational processes in breast cancer. *Nature* 2012;486:400-4.
 38. Modhukur V, Iljasenko T, Metsalu T, et al. MethSurv: a web tool to perform multivariable survival analysis using DNA methylation data. *Epigenomics* 2018;10:277-88.
 39. Liu J, Lichtenberg T, Hoadley KA, et al. An Integrated TCGA Pan-Cancer Clinical Data Resource to Drive High-Quality Survival Outcome Analytics. *Cell* 2018;173:400-416.e11.
 40. Lániczky A, Györfy B. Web-Based Survival Analysis Tool Tailored for Medical Research (KMplot): Development and Implementation. *J Med Internet Res* 2021;23:e27633.
 41. Fekete JT, Györfy B. ROCplot.org: Validating predictive biomarkers of chemotherapy/hormonal therapy/anti-HER2 therapy using transcriptomic data of 3,104 breast cancer patients. *Int J Cancer* 2019;145:3140-51.
 42. Uhlén M, Björling E, Agaton C, et al. A human protein atlas for normal and cancer tissues based on antibody proteomics. *Mol Cell Proteomics* 2005;4:1920-32.
 43. Uhlen M, Zhang C, Lee S, et al. A pathology atlas of the human cancer transcriptome. *Science* 2017;357:eaan2507.
 44. Györfy B. Survival analysis across the entire transcriptome identifies biomarkers with the highest prognostic power in breast cancer. *Comput Struct Biotechnol J* 2021;19:4101-9.
 45. Wang N, Eckert KA, Zomorodi AR, et al. Down-regulation of HtrA1 activates the epithelial-mesenchymal transition and ATM DNA damage response pathways. *PLoS One* 2012;7:e39446.
 46. Franco R, Collina F, Di Bonito M, et al. HtrA1 loss is related to aggressive behavior parameters in sentinel node positive breast cancer. *Histol Histopathol* 2015;30:707-14.
 47. Wei LY, Zhang XJ, Wang L, et al. A Six-Epithelial-Mesenchymal Transition Gene Signature May Predict Metastasis of Triple-Negative Breast Cancer. *Oncotargets Ther* 2020;13:6497-509.
 48. Tang T, Zhu Q, Li X, et al. Protease Nexin I is a feedback regulator of EGF/PKC/MAPK/EGR1 signaling in breast cancer cells metastasis and stemness. *Cell Death Dis* 2019;10:649.
 49. Harbeck N, Penault-Llorca F, Cortes J, et al. Breast cancer. *Nat Rev Dis Primers* 2019;5:66.
 50. Denkert C, von Minckwitz G, Darb-Esfahani S, et al. Tumour-infiltrating lymphocytes and prognosis in different subtypes of breast cancer: a pooled analysis of 3771 patients treated with neoadjuvant therapy. *Lancet Oncol* 2018;19:40-50.
 51. Emens LA, Cruz C, Eder JP, et al. Long-term Clinical Outcomes and Biomarker Analyses of Atezolizumab Therapy for Patients With Metastatic Triple-Negative Breast Cancer: A Phase 1 Study. *JAMA Oncol* 2019;5:74-82.
 52. Terranova-Barberio M, Pawlowska N, Dhawan M, et al. Exhausted T cell signature predicts immunotherapy response in ER-positive breast cancer. *Nat Commun* 2020;11:3584.
 53. Folgueira MA, Carraro DM, Brentani H, et al. Gene expression profile associated with response to doxorubicin-based therapy in breast cancer. *Clin Cancer Res* 2005;11:7434-43.
 54. Carrara GFA, Evangelista AF, Scapulatempo-Neto C, et al. Analysis of RPL37A, MTSS1, and HTRA1 expression as potential markers for pathologic complete response and survival. *Breast Cancer* 2021;28:307-20.

Cite this article as: Zhao D, Li W, Wang Y, Zhang G, Bai X, Yu H. HTRA1 expression is associated with immune-cell infiltration and survival in breast cancer. *Transl Cancer Res* 2023;12(12):3503-3521. doi: 10.21037/tcr-23-773